

A multianalytical approach to investigate stone biodeterioration at a UNESCO world heritage site: the volcanic rock-hewn churches of Lalibela, Northern Ethiopia

Nick Schiavon · Tilde De Caro · Alemayehu Kiros ·
Ana Teresa Caldeira · Isabella Erica Parisi ·
Cristina Riccucci · Giovanni Ettore Gigante

Received: 16 April 2013 / Accepted: 30 April 2013 / Published online: 22 May 2013
© Springer-Verlag Berlin Heidelberg 2013

Abstract A multianalytical approach combining Optical Microscopy (OM), Backscattered Variable Pressure Scanning Electron Microscopy + Energy Dispersive X-ray Spectroscopy (VP-BSEM + EDS), Powder X-ray Diffractometry (PXRD), Raman Spectroscopy, and Microbiological techniques has been applied to characterize decay products and processes occurring at the surface of two rock-hewn churches (*Bete Gyorgis and Bete Amanuel*) at the UNESCO's World Heritage site of Lalibela, Northern Ethiopia. The two churches were carved into volcanic scoria deposits of basaltic composition. In their geological history, the Lalibela volcanic rocks underwent late to post-magmatic hydrothermal alteration together with partial laterization and are therefore characterized by a decay-prone highly vesicular microtexture with late stage to post-magmatic precipitation of secondary mineral phases (calcite–zeolite–smectite). The main objective of the study was to gain a better insight into the weathering products and mechanisms affecting the surface of the stone monuments and to assess the relative

contribution of natural “geological” weathering processes versus biological/salt attack in stone decay at this unique heritage site. Results indicate that while the main cause of bulk rock deterioration and structural failure could be related to the stone inherited “geological” features, biological attack by micro- (bacteria) and/or macro- (lichens) organisms is currently responsible for severe stone surface physical and chemical weathering leading to significant weakening of the stone texture and to material loss at the surface of the churches walls. A prompt and careful removal of the biological patinas with the correct biocidal treatment is therefore recommended.

1 Introduction

The Lalibela UNESCO World Heritage site is located near the rural town of Lalibela, 600 km north of Addis Ababa, in Northern Ethiopia at an altitude of 2500 m above s.l. The town has 12.000 inhabitants and hosts a unique complex of eleven rock-hewn churches (Fig. 1) believed to have been carved in the 12th century A.D. by the King Lalibela (1167–1207) of the Zagwe dynasty [1]. The churches are still used today for religious practices and ceremonies, and on the occasion of major religious events, large crowds of believers and pilgrims gather at the site mingling with an increasing flux of foreign tourists. According to their geographical distribution (Fig. 1), the churches are traditionally subdivided into three main groups: the first one comprises 6 churches, i.e., *Bete Medhane Alem (Church of the Holy Saviour)*, *Bete Marian (St. Mary's Church)*, *Bete Mesqel (Church of the Cross)*, *Bete Denagel (Virgins Church)*, *Bete Debre Sina (Mount Sinai Church)*, and *Bete Golgotha (Golgotha Church)*; the second one comprises 4 churches, i.e., *Bete Gabriel-Rufael (Church of S. GabriellRafael)*, *Bete*

N. Schiavon (✉)
HERCULES Laboratory and Évora Geophysics Centre (CGE),
University of Évora, Évora, Portugal
e-mail: schiavon@uevora.pt

T. De Caro · I.E. Parisi · C. Riccucci
CNR-ISMN, Rome, Italy

A. Kiros
Department of Physics, University of Addis Ababa, Addis Ababa,
Ethiopia

A.T. Caldeira
Department of Chemistry, University of Évora, Évora, Portugal

G.E. Gigante
Department SBAI, Sapienza University of Rome, Rome, Italy

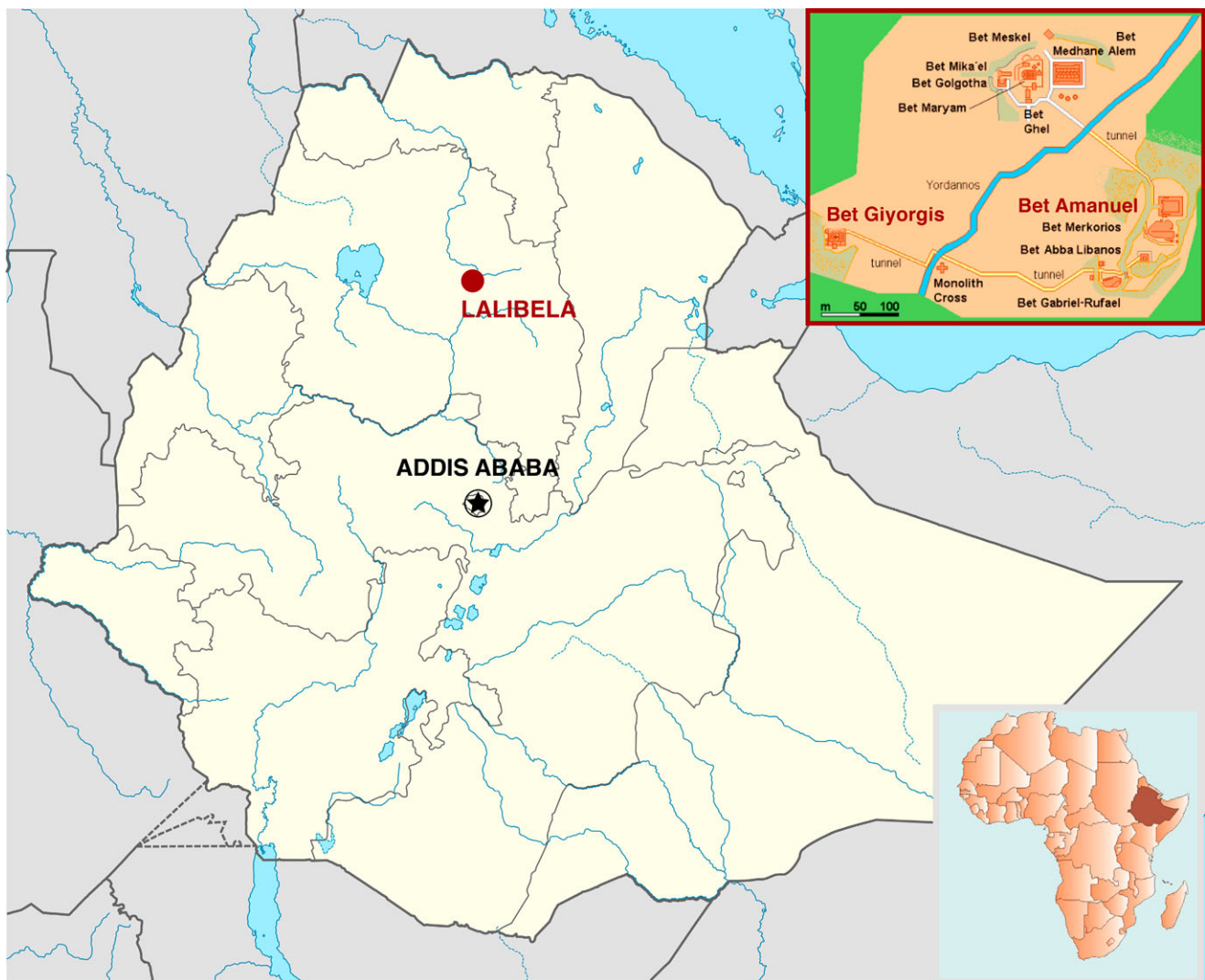


Fig. 1 Lalibela location map. *Inlet (top right)* shows the geographical distribution of the rock-hewn churches at the Lalibela monumental site

Amanuel (St. Emmanuel Church: Fig. 2), *Bete Merkorios* (St Mark's Church), and *Bete Abba Libanos* (Father Libanos Church), while the third group is represented by only one, isolated, church (perhaps the most iconic one), i.e., *Bete Gyorgis* (S. George's Church: Fig. 2). From an architectural of view, three modes of construction were used: (a) built-up churches inside existing natural caves (e.g., *Bete Merkorios*); (b) quarried enlargement and rock-hewn churches of an existing vertical cliff face (e.g., *Bete Medhane Alem*); (c) monolithic rock-hewn churches carved as one piece into the surrounding bedrock and separated by trenches all round the monument, e.g., *Bete Gyorgis* and *Bete Amanuel*, Fig. 2). The churches are often interconnected with each other through a maze of underground tunnels and passages.

Northern Ethiopia's geology is characterized by thick sequences of tholeiitic to transitional continental flood basalts overlain by minor rhyolitic–trachytic lavas and pyroclastic rocks of Oligocene to Miocene belonging to the Northern

Ethiopian Plateau [2–5]. Within the plateau, three magma types have been distinguished: two high-Ti groups (HT1 and HT2), and one low-Ti group (LT). The central-eastern sector of the plateau in particular, i.e., the one comprising the Lalibela area and facing the Afar triangle, is mainly characterized by a 1700 m-thick sequence of high TiO_2 (HT2 magma type) picrite/basalt lavas capped by about 300 m of rhyolites, linked to the magmatic activity at the Afar plume axial zone [3]. The HT2 volcanics [2] are represented by subalkaline olivine-clinopyroxene aphyric or glomerophyric basalts and picrites with phenocrysts of euhedral olivine (FO_{86} – FO_{81} range) and of Mg–Ti–Al rich augite. The groundmass contains olivine, clinopyroxene, Fe–Ti oxides and plagioclase (An_{85} – An_{48} range) microlites. The Oligocene volcanism of the northwestern Ethiopian Plateau has been subdivided into three formations [6]; the Ashangi and Amba Aiba basaltic units, separated by an angular unconformity [7] from the upper ignimbritic Alaji unit. In the Lalibela mon-

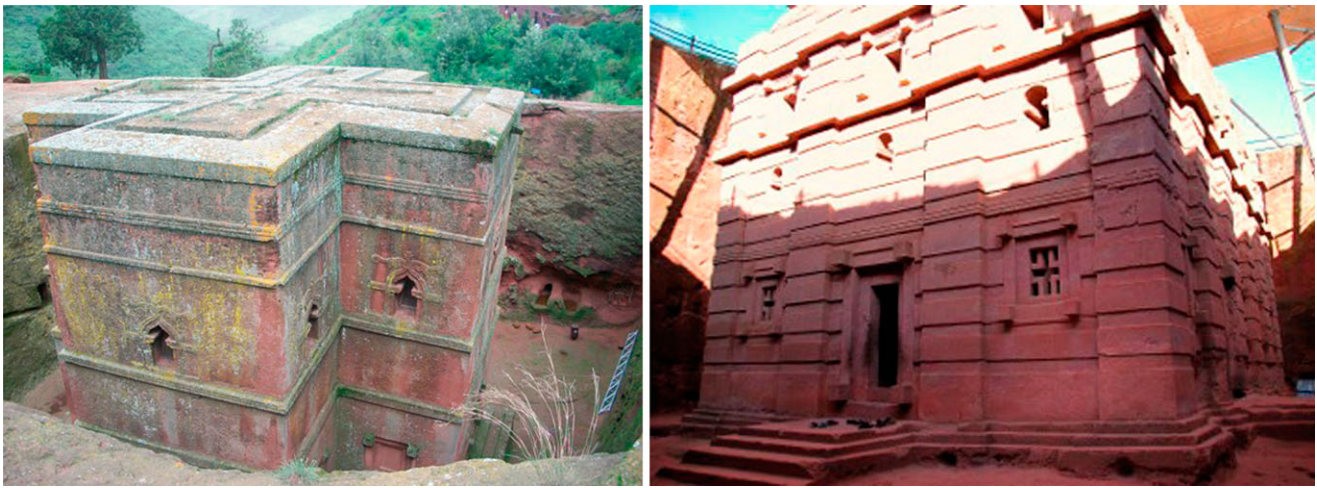


Fig. 2 Sampling sites. *Bete Gyorgis* (left) with widespread lichenous cover and *Bete Amanuel* (right)

umental site, the Amba Aiba basalts are typically overlain by a thick horizon of reddish highly hydrothermally weathered basaltic scoria (commonly referred to as “tuffaceous material”). It is within this “softer” unit that the rock-hewn churches were carved.

In the past 30 years (mainly as a result of initiatives led by international Cultural Heritage Institutions such as ICROM, WHF, UNESCO, WHC), the Lalibela monumental complex has been the subject of several studies sharing the common objective of assessing the main factors leading to the severe stone decay observed at this unique urban site. Among these factors, the widespread presence of fractures and discontinuities within the basaltic scoria allowing percolation through the rock mass of surface water [8], which coupled with extensive groundwater seepage [5, 9, 10] leads to potential slope/structure failure, the mechanical erosion due to rain drops and wind [9], and the hydrothermally induced mineral reactions within the highly porous volcanic scoria deposits leading to montmorillonite and zeolite precipitation with associated cycles of water absorption/desorption [9–11], have been indicated as the main decay mechanisms.

These studies have prompted the Ethiopian government to construct temporary shelters over selected heavily damaged churches (Fig. 2) in order to protect the churches from direct rainwater impact [12, 13]. The effectiveness of these interventions both from a conservation as well as an aesthetic perspective though have been recently seriously questioned [14]. On the other hand, salt weathering processes, and in particular biological activities, although noted, have never been indicated as a major decay threat nor have been studied in detail [5, 8, 10, 11]. This is somewhat surprising as widespread biological cover (mainly by saxicolous crustose lichens) is readily visible and evident at a macroscopic level on many churches facades (in particular at the Bete Gyorgis church site; Fig. 2). It is well known that underneath often continuous and apparently undisturbed lichenous mats



Fig. 3 Bete Amanuel side wall. Note extensive biological colonization by lichens and mosses

in both urban and natural environments, intense decay leads to weakening and enhanced material loss not only on “softer” lithotypes such as limestones [15–17] but also on “harder” silicate stones such as, for example, granites [16, 18–20], basalts [21, 22], and ultramafic rocks [23].

The aim of the present study was therefore to study in detail for the first time, using a multi-analytical approach combining Optical Microscopy (OM), Backscattered Variable Pressure Scanning Electron Microscopy + Energy Dispersive X-ray Spectroscopy (VP-BSEM + EDS), Powder X-ray Diffractometry (PXRD), Raman Spectroscopy, and standard Microbiological Techniques, the biodeterioration processes and products associated with lichenous coatings on a “unusual” building stone such as the Lalibela volcanic scoria with a view to be able to contribute to a better conservation strategy for this World Heritage site. Two monumental sites in the Lalibela site characterized by a widespread lichen cover were selected for investigation: *Bete Gyorgis* and *Bete Amanuel* churches (Figs. 2, 3).

2 Materials and methods

Small fragments were carefully sampled from internal and/or external walls of selected Lalibela churches. In particular, ground fallen samples from the tunnel wall at the east side of *Bete Amanuel* church facing the church's gate were collected together with samples from the rock-hewn wall near *Bete Gyorgis* church. Additional samples were also collected from the Mahilet rock hewn cave situated on the right side of *Bete Gyorgis* gateway. Samples were collected by one of the authors (AK) following the authorization of the Ethiopian government.

The samples were submitted to analyses according to the specific requirements of the following analytical techniques: X-ray diffraction (XRD), micro-Raman spectroscopy (μ -Raman), optical microscopy (OM), scanning electron microscopy (SEM) with backscattered and secondary electron imaging and energy dispersive spectrometry (EDS), and microbiological characterization.

In order to prepare cross-section, some fragments were embedded in epoxy resin for 24 hours and sectioned by using a diamond saw in order to preserve the structural and chemical features of the materials. The sections were polished with silicon carbide papers up to 1200 grit and the final polishing was performed with diamond pastes up to $\frac{1}{4}$ μm in order to have mirror like surfaces. 30 micron-thick thin sections were made after embedding stone fragments (2×1 cm) in epoxy resin.

Glass slides were examined, under transmitting light, with a polarizing Leica optical microscope for stone petrographical-mineralogical characterization [24, 25].

X-ray diffraction patterns were recorded directly both on stone fragments and on powders (50–100 mg). Diffraction patterns were recorded by a Siemens 5000 X-ray powder diffractometer with Ni-filtered $\text{Cu K}\alpha$ radiation ($\lambda = 0.154056$ nm) using the following experimental conditions: 2θ angular values between 5° and 80° in additive mode; a step size of 0.05° 2θ and a sampling time of 20 s. X-ray diffraction patterns were analyzed using X-Pert electronic databases.

The surface morphology was observed by using a Leica MZ FLIII and a multifocus Leica optical microscopes equipped with a digital camera.

BSEM-EDS investigation was carried out by a Variable Pressure HITACHI S3700N Scanning Electron Microscope interfaced with a Bruker Quantax microanalysis system. The Quantax system was equipped with a Bruker AXS X-Flash[®] Silicon Drift Detector (129 eV Spectral Resolution at FWHM— $\text{Mn K}\alpha$). Standardless PB/ZAF quantitative elemental analysis was performed using the Bruker ESPRIT software. The operating conditions for EDS analysis were as follows: backscattered electron mode (BSEM), 20 kV accelerating voltage, 10 mm working distance, 120 mA emis-

sion current. Samples were coated with a thin layer of carbon in order to avoid charging effects. The carbon coating was obtained using an Emitech sputter coater K550 unit, a K 250 carbon coating attachment and a carbon cord at a pressure of 1×10^{-2} mbar in order to produce a carbon film with a constant thickness of about 3.0 nm. These conditions have proven optimal to investigate the interface decay patinas/substrate in a variety of historic materials [26–31].

Micro-Raman characterization was performed using a Renishaw 2000 μ -Raman instrument equipped with a Peltier refrigerator-cooled charge-coupled device (CCD) camera in conjunction with a Leica optical microscope. The laser was focused on the sample through a $\times 100$ or $\times 50$ objective lenses. The excitation light was the 514.5 nm line of an Ar^+ laser and a 785 nm line of a diode laser with laser power in the range of 10–60 μW . The typical spectrometer resolution was about 2 cm^{-1} .

To investigate microbiological colonization, samples from *Bete Gyorgis* and *Bete Amanuel* stones were sampled under aseptic conditions, using cotton buds diluted in 1 ml of sterile maximum recovery diluent and shaken mechanically for 1 h. Serial dilutions in peptone saline diluent were used to prepare Nutrient Agar (NA) plates. Bacterial isolation procedures were carried out in Petri dishes containing NA supplemented with 0.005 % cycloheximide at 30°C , for 48 hours. The distinct single colonies obtained were subcultured onto NA for characterization. Bacterial strains were maintained on NA slants at 4°C . Fungal isolation of the colonies was done successively, using standard mycological medium (Malt extract agar, Potato-dextrose agar, and Cook Rose Bengal). All cultures were grown for 7 days at 28°C . Macroscopic and microscopic characteristics of the obtained isolates were examined. Identification of fungi was based on the macroscopic features of colonies grown on agar plates, and the micromorphology of the reproductive structures was identified by OM and VP-SEM-EDS. Samples for scanning electron microscopy (SEM) were air-dried, coated with gold and examined in the Hitachi Scanning Electron Microscope S-3700N taking advantage of its low-vacuum setting enabling to observe biological attack without the need for C or Au sputtering. The accelerating voltage was 18–20 kV.

3 Results

The rock texture is characterized by abundant vesicles and open voids readily visible under both OM and BSEM examination (Figs. 4, 5) and occupying about 40–50 % of the stone volume. This is reflected in the stone high porosity (ranging from 13.5 to 36 %—average 28 %) and low apparent density (γ_d ranging from 1.75 to 1.99 gr/cm^3 —average 1.83 gr/cm^3), which in turn are indicative of nat-

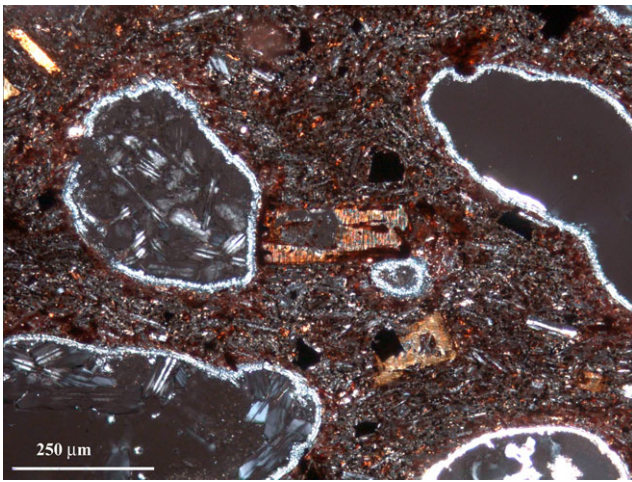


Fig. 4 Petrography–OM/Nx. Highly vesicular basaltic scoria of low porphyritic index with vesicles filled with euhedral zeolites and microphenocrysts of clinopyroxenes in a microlitic groundmass

ural stone weathering mechanisms active during the Lalibela basaltic scoria geological history. Vesicles are often fully and/or partly filled with secondary minerals resulting from hydrothermal, syn-postmagmatic precipitation by hot fluids penetrating through the highly permeable pyroclastic scoria deposits from the underlying basaltic lava flows: of particular relevance is the widespread occurrence of zeolite-group minerals, i.e., pseudo-cubic to massive analcite ($(\text{Na}_{16}[\text{Al}_{16}\text{Si}_{32}\text{O}_{96}] \cdot 16\text{H}_2\text{O})$; Fig. 5b), acicular natrolite ($(\text{Na}_{16}[\text{Al}_{16}\text{Si}_{24}\text{O}_{80}] \cdot 16\text{H}_2\text{O})$; Fig. 5c) and platy/coffin shaped heulandite-Ca $[(\text{Ca},\text{Na})_{2-3}\text{Al}_3(\text{Al},\text{Si})_2\text{Si}_{13}\text{O}_{36} \cdot 12\text{H}_2\text{O}]$; Fig. 5d) often associated with well developed euhedral calcite with its typical rhombic cleavage (Fig. 5e) and with platelets of phyllosilicates belonging to the smectite group (Fig. 5f). In terms of bulk petrography, the volcanic scoria deposits display a microlitic (rarely aphyric) texture with low porphyritic index (phenocrysts always <5 vol%, often <1 vol%) characterized by euhedral to subhedral hydrothermally altered and oxidized microphenocrysts (grain size never >1 mm and averaging 0.5 mm) of prismatic clinopyroxenes (often associated with Fe/Ti oxides to form glomerocrysts; Fig. 6a), Ca-plagioclases (An_{85-65}), Fe–Ti oxides and rare, highly altered (laterized) olivine. The clinopyroxenes are mostly of augitic composition showing high Mg and Ti contents together with low Si/Al ratios and are frequently highly altered and oxidized (Fig. 6b). The Fe/Ti rich oxides are mainly composed by Ti-hematite with typical martite “trellis” texture (common in hydrothermally altered volcanics and derived from hydrothermally induced alteration as relics of magnetite-ulvospinel solid solution minerals; Fig. 6a), ilmenite, Ti-magnetite with inter-lamellae of ilmenite, and ulvospinel. The microcrystalline to cryptocrystalline fine-grained groundmass display a mainly hyalop-

ilitic, locally eutaxitic (i.e., showing banded features typical of volcanic deposits) texture and is composed mainly by intergranular microlitic laths of plagioclase feldspars and clinopyroxene (Fig. 6c), and by equant mineral grains of Fe–Ti oxides dispersed into a Fe-rich glassy matrix (Fig. 6d).

XRD data on whole rock samples confirm the presence of peaks attributable to zeolites (in order of peak strength: analcime, heulandite, thomsonite, wairakite, polucite, clinoptilite, scolecite), clinopyroxenes, hematite, calcite, magnetite and minor smectites. The strongest Fe oxide peaks detected are those of hematite although poorly defined peaks of ilmenite are also present: this evidence combined with the BSEM + EDS data (Fig. 6a) confirms that the main crystalline form of these oxides is Ti-hematite. Ca-oxalate peaks attributable to weddellite, although present in a few samples, are rare and poorly defined indicating a low crystallinity index for these oxalates. Micro Raman on the microlitic groundmass confirmed the extensive laterization experienced by the basaltic pyroclastic scoria deposit with the identification (beside peaks attributable to zeolitic minerals) of well-defined peaks of hematite, lepidocrocite, and combined hematite/lepidocrocite (Fig. 7).

BSEM + EDS investigation of rock samples with surface lichen patinas from the two investigated sites highlights the decay features and processes associated with bio-colonization of the Lalibela pyroclastic/volcanic stone (Fig. 8). Lichenous patinas vary in thickness between 100 and 500 μm (Figs. 8a, 8b) but lichen’s hyphae are able to take advantage of the stone high porosity texture and penetrate at even greater depths within the stone substrate through the often interconnecting network of vesicles and preexisting cracks: in fact, evidence of lichen activity and of the presence of algal filaments may be found up to several cm deep from the rock-lichen interface (Fig. 8c). It is interesting to note how lichen’s hyphae penetration seem also to occur via intercrystalline porosity in the groundmass regardless of the presence of preferential lines of weakness (Fig. 8d). BSEM investigation of the interface lichenous patina/stone substrate clearly reveals how, underneath the biological mat cover, the volcanic scoria substrate is undergoing extensive mineral disaggregation eventually leading to incorporation of the detached mineral fragments within the biological patina (Fig. 8b). The bio-mediated decay is not only of a physical nature: evidence for intracrystalline corrosion/replacement of mineral grains, in particular microphenocrysts of clinopyroxene, is frequently found (Figs. 8e, 8f) as is the occurrence of biofilms, probably of polysaccharide nature, coating phenocrysts and/or embedding mineral grains (in particular Fe-oxides; Fig. 8g) in the microcrystalline groundmass.

The microbiological study on samples from both investigated sites allowed the isolation of 11 bacterial strains (e.g.,

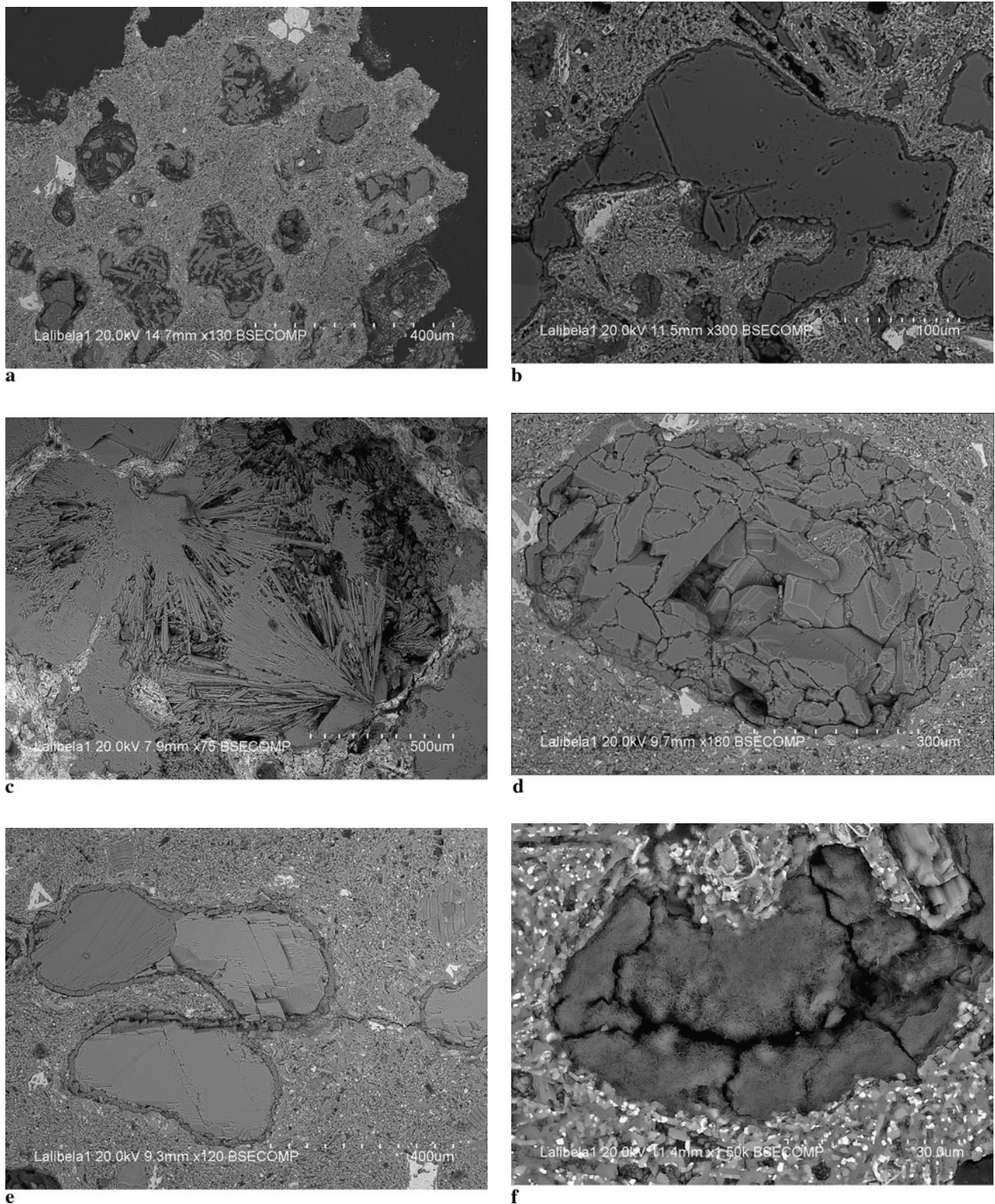


Fig. 5 Petrography–BSEM. **(a)** General view of the volcanic basaltic scoria underneath a lichenous patina (*bottom right*) highlighting the presence of microphenocrysts of clinopyroxenes and Fe–Ti rich oxides in a plagioclase/clinopyroxene/Fe-rich groundmass and of zeolite filled vesicles; **(b)** vesicle-filling anhedral analcime; **(c)** vesicle-

filling acicular natrolite; **(d)** vesicle-filling heulandite with typical prismatic (“coffin shaped”) habit; **(e)** general view showing associated calcite (rhombic cleavage)/heulandite vesicle-filling; **(f)** vesicle-filling smectitic clay

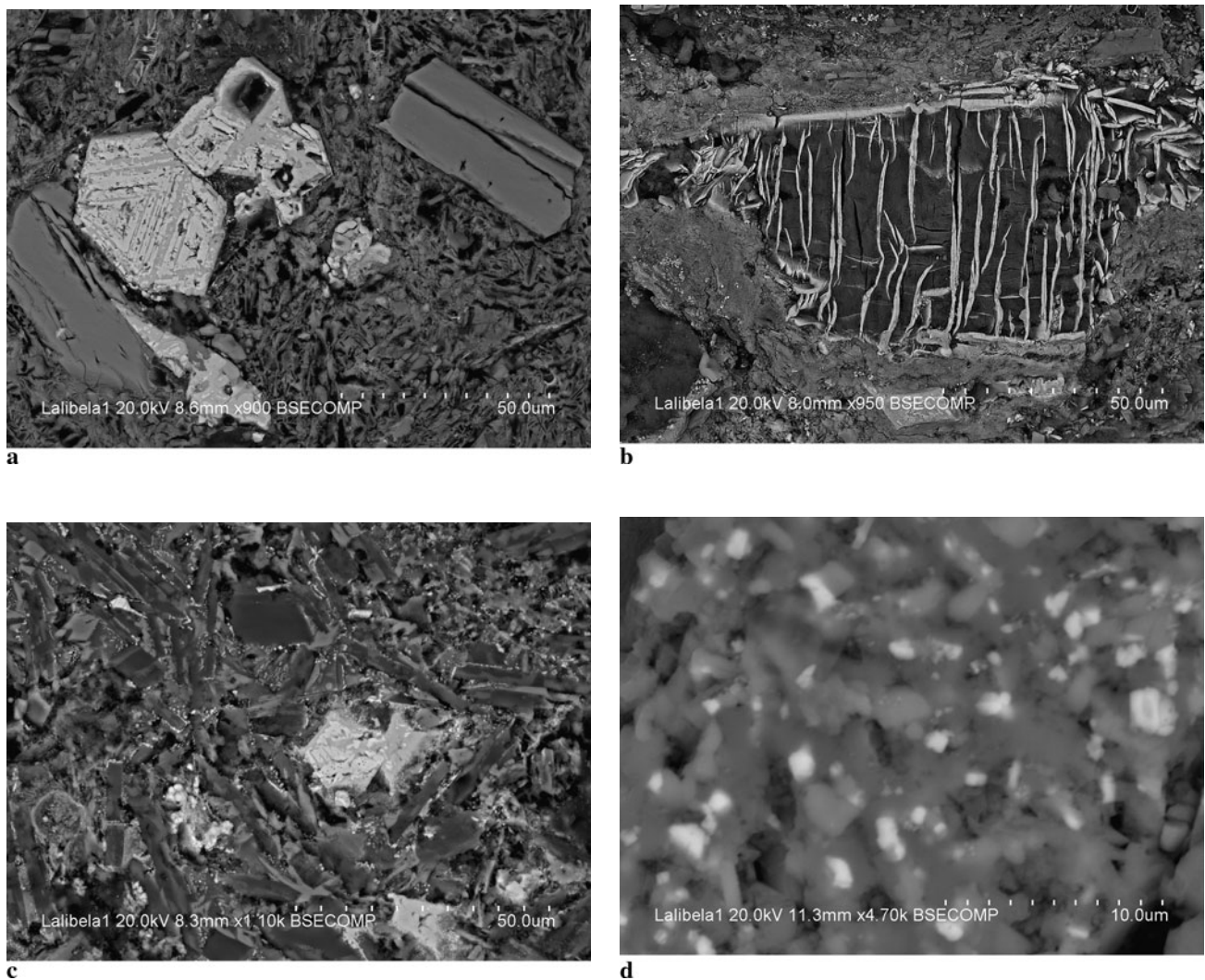


Fig. 6 Petrography–BSEM. **(a)** Microphenocrysts of clinopyroxene (darker) and of Fe–Ti oxides (brighter) showing martite “trellis” texture (common in hydrothermally altered volcanics); **(b)** highly altered and oxidized clinopyroxene showing preferential etching along cleav-

age planes; **(c and d)** close-ups of groundmass composed mainly by intergranular microlitic laths of plagioclase feldspars and clinopyroxene and equant mineral grains of Fe–Ti oxides dispersed into a Fe-rich glassy matrix

Gram+ cocci, Gram+ bacilli, 2 yeast strains and 10 filamentous fungi strains (Fig. 9a). The most predominant genera were *Penicillium*, *Cladosporium*, and *Aspergillus* sp. and sterile mycelia. LV-SEM examination confirms widespread biological contamination of the scoriaceous basaltic samples (Fig. 9b).

4 Discussion

Microscopical and petrographical investigation by OM and VP-BSEM + EDS confirms that the Lalibela churches were carved into highly vesicular, hydrothermally weathered, and partly laterized pyroclastic scoria deposits of basaltic composition. The results together with the observed

mineral paragenesis are consistent with published petrographical/geochemical compositional data of Lalibela volcanics, and in particular of the HT2 transitional basalts group of the NW Ethiopian plateau [2, 3]. The presence in the stone of plagioclase feldspars both as phenocrysts (rare) and as microlitic laths in the groundmass (common) rules out the identification of the basaltic rocks as limburgites as suggested in a previous study [5], but rather points to a porphyritic basaltic rock. In this study, though, lower amounts of olivine phenocrysts have been detected as compared with typical Ethiopian HT2 basalts and indeed no peaks unequivocally ascribable to olivine have been found in the XRD analyses: this can be due to the highly hydrothermally altered nature of the olivine crystals that are often almost completely altered (laterized) to secondary Fe-rich oxide-

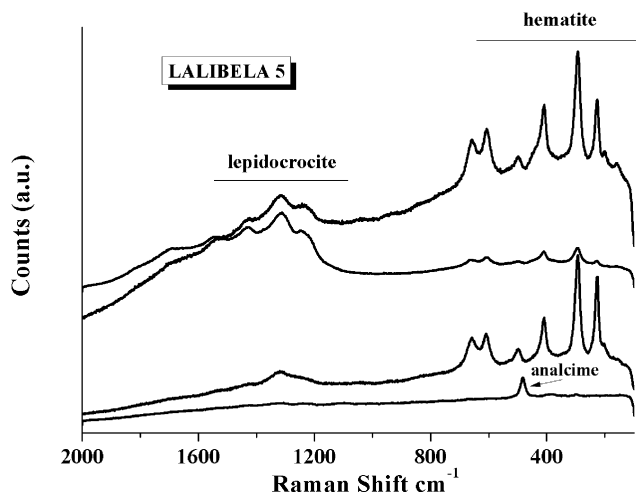


Fig. 7 Micro-Raman. Typical micro-Raman spectrum of the Lalibela basaltic scoria groundmass

hydroxides. The petrographical results in this study are also in agreement with mineral-petrographical and/or geochemical analyses of volcanic rocks of the rock-hewn churches sites [8, 11] and contributes toward a more precise petrographic classification of the Lalibela's stones previously quoted using a somewhat confusing variety of lithological names such as welded ignimbrites, weathered red tuffs or, more vaguely, as tuffaceous material *s.l.* [5].

The widespread, abundant presence within the stone fabric of secondary minerals belonging to the zeolite and smectite groups has had important bearings on the stone susceptibility to weathering. In fact, the well recognized property of these hydrated aluminosilicates to adsorb/desorb water reversibly and to exchange cations with water solutions due to the presence in their crystalline framework of interlinked cages and channels large enough to host exchangeable small molecules (such as water) and cations has already been suggested as one of the main causes of stone weathering in the Lalibela rock-hewn churches [10, 11]. Notwithstanding the important role of the zeolitic and smectitic mineral components in the decay of the Lalibela volcanic scoria lithology into which the churches have been carved, though, this study highlights for the first time the major role played by epilithic and endolithic lichen colonization in the weathering of the Lalibela stones. One of the intensively biocolonized churches investigated, i.e., *Bete Gyorgis*, had been previously quoted as being the “least affected by man-made and natural decay factors” and an “almost intact rock” with reported rock strength range of 75–83 MPa and a Rock Mass Rating [32] of 92 [5, 33]. These measurements were, though, referring to the bulk rock and not to its surface where the effects of the biocolonization are most intensive. In fact, underneath the widespread and fairly continuous lichenous mats coating almost the whole surface of the Lalibela volcanic scoria deposits in the two investigated churches, both

biogeophysical and *biogeochemical* processes appear to be highly active in synergistically causing severe degradation. It is important to note that these biomediated decay processes are not restricted to the outermost interface stone-atmosphere, but are active deep within the stone substrate.

Biogeophysical decay operates through the following two main mechanisms: (a) hyphae mechanical substrate penetration through turgor pressures associated with expansion and contraction wet–dry cycles in the lichen thalli affecting its gelatinous or mucilaginous substances. The biomediated excretion of extracellular polymeric substances (EPS: polysaccharides, lipopolysaccharides, proteins, glycoproteins, lipids, glycolipids, fatty acids and enzymes) also results in mechanical stresses to the rock structure due to shrinking and swelling cycles of the colloidal biogenic slimes inside the pore system [34]. This leads to the alteration of the stone's pore size distribution and result in changes of moisture circulation and temperature gradient patterns. The mechanical action of lichen thalli on the rock generally consists of an extensive disaggregation and fragmentation of the lithic surface immediately below the lichen crust with incorporation of mineral fragments into the growing biological patina (Figs. 8a, 8b); the ease and degree of hyphae penetration within the stone substrate is largely controlled by the physicochemical properties of the rock, i.e., compactness, hardness, lamination, or preexisting surface alteration [35]. The abundant vesicle network with associated high porosity, which is typical of volcanic scoria deposits such as the ones used to excavate and build the unique Lalibela monuments has been widely recognized to allow lichen's organs to penetrate very deep within the substrate framework. In the colonization of leucite-bearing volcanic rocks near Mt St. Vesuvius in Italy, for instance, the organ of adhesion of the lichen *Stereocalium vesuvianum*, the pseudopodium, and its ramifications has been found up to a depth of 30 mm within the rock substrate; likewise, in Lalibela, unequivocal evidence for hyphae penetration has been found down to several millimeters from the basaltic scoria church wall/atmosphere interface (Fig. 8c); (b) microbial biofilms (which more than often act as precursors to the subsequent development of stone surface covering lichenous mats and are widespread in Lalibela, Fig. 8g) modify the capillary water uptake of porous stone material causing measurable alterations in the water-vapor diffusion properties of the lithic material. Furthermore, the water and moisture retention properties of the lichen patinas may enhance physical decay stresses associated with naturally occurring freeze-thaw cycles. In urban, polluted environments, biofilms have also been found to enhance the dry/wet deposition of atmospheric gaseous and particulate pollutants on outdoor stone facades [36, 37], thus playing a role in the biomediated precipitation of sulfate compounds such as gypsum and providing an additional route for salt weathering

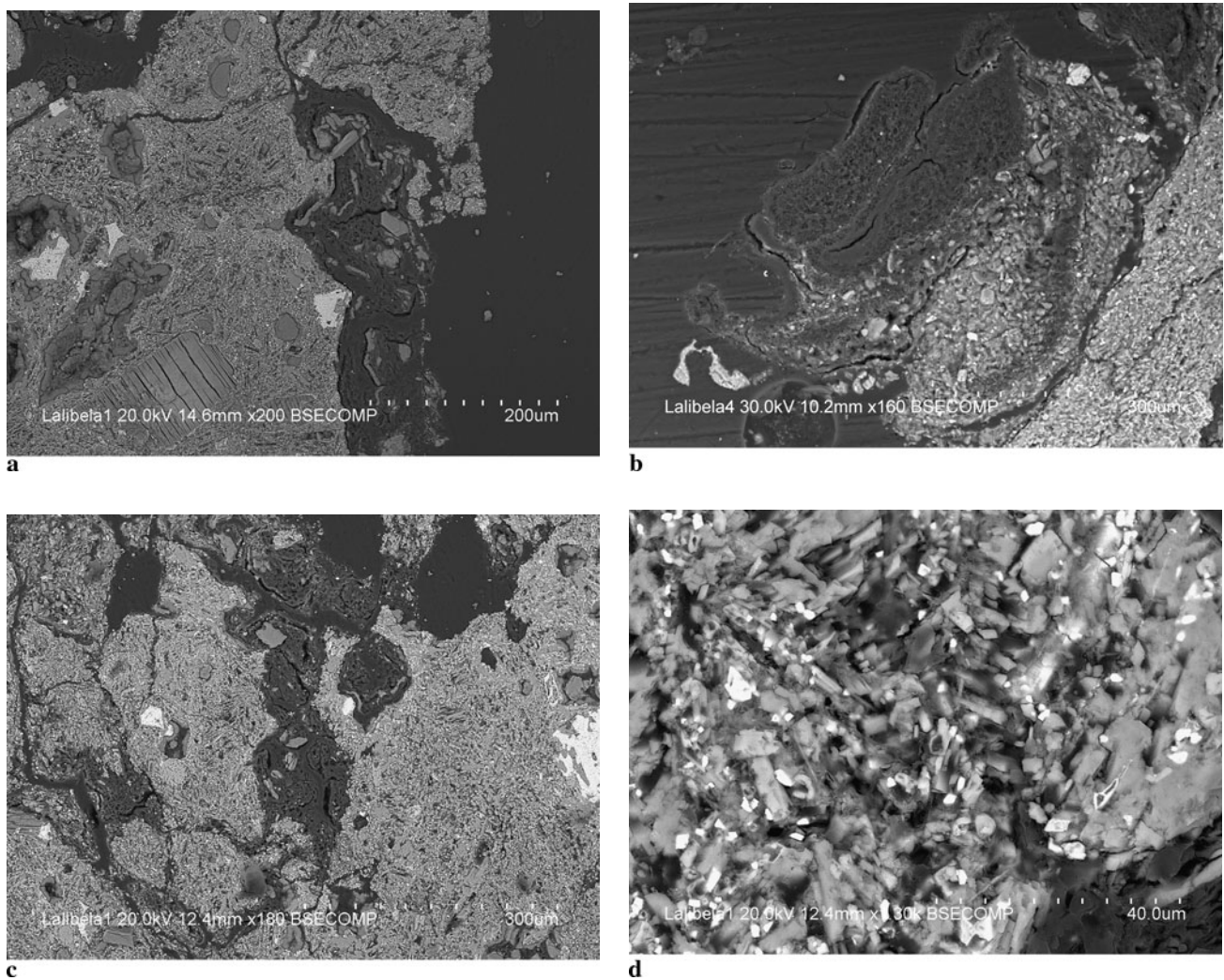


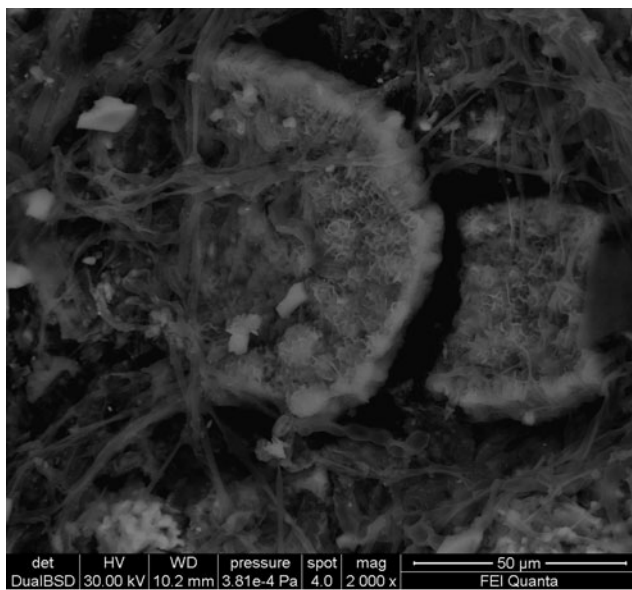
Fig. 8 Biodeterioration—BSEM. (a) Interface stone/lichenous patina showing penetration and bio-corrosion; (b) Thick bio-patina with active desegregation and incorporation of mineral fragments from underlying rock substrate; (c) physical penetration of lichen's hyphae deep within the stone substrate exploiting and enlarging pre-existing frac-

tures and porosity; (d) close-up of microlitic groundmass showing intercrystalline hyphae penetration; (e) deep etching and bio-corrosion of clinopyroxene mineral grain; (f) intracrystalline biological attack on clinopyroxene mineral showing both physical and chemical decay; (g) biofilm (EPS) coating crystalline Fe/Ti oxides

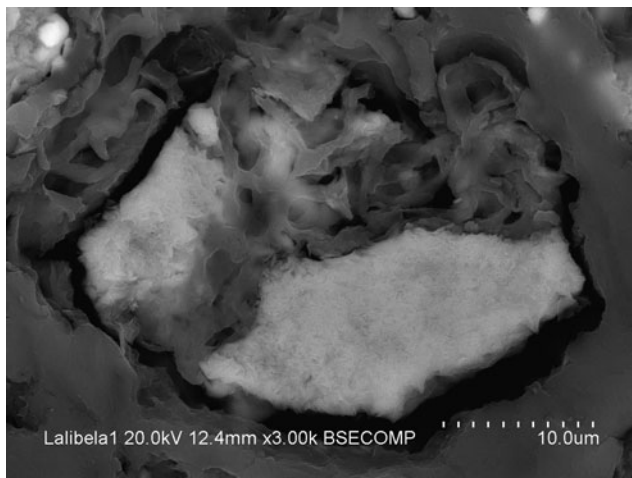
decay and growth of surface weathering black crusts [16]. Microbial contamination may act indeed as a preliminary precursor for the formation of detrimental crusts on rock surfaces caused by the acidolytic and oxido-reductive (bio) corrosion activities on mineral structures [16–20]. In the Lalibela monumental site, though, SO_2 and/or vehicular exhaust emissions-linked air pollution does not seem to represent (at least for the moment) a major issue in the area as a local environmental review quoting only wood burning and/or solid waste as potential threats to the Lalibela environment recently concluded [38]. Correspondingly, also the content of air pollution derived salts (sulphates, nitrates) within the stone has been found to be quite low [11].

Beside decay driven by biogeophysical processes, analytical/microscopical evidence clearly suggests that *biogeo-*

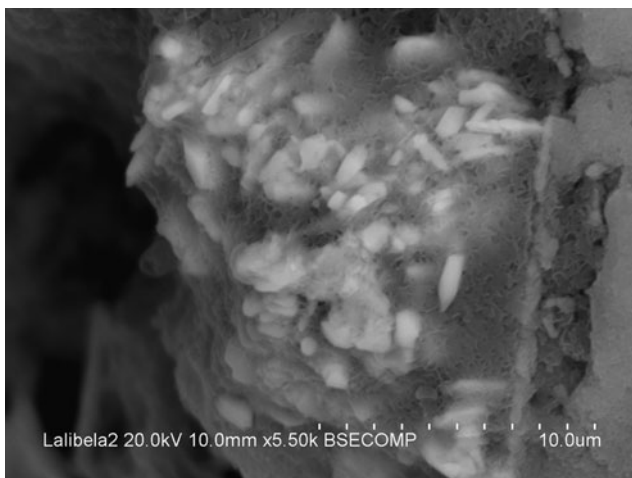
chemical weathering also play a major role in the deterioration of the volcanic stone in the Lalibela monuments. Again, two main mechanisms (often acting simultaneously) may be envisaged: acidolysis/dissolution and metal complexation [35, 39]. The excretion by the mycobiont of lichens of low molecular weight organic carboxylic acids, such as oxalic, citric, gluconic, lactic acids, with combined chelating and acidic properties, and the production of slightly water soluble polyphenolic compounds called “lichen acids,” are processes known to lead to the formation of complexes with the metal cations (such as Mg^{++} and Fe^{++}) in rock-forming minerals, eventually leading to their extraction by chelation to be used as nutrients and energy suppliers both by micro (bacteria) and macro (lichen) organisms [34, 35, 39]. The chelation of metals by organic ligands is also known to in-



e



f



g

Fig. 8 (Continued)

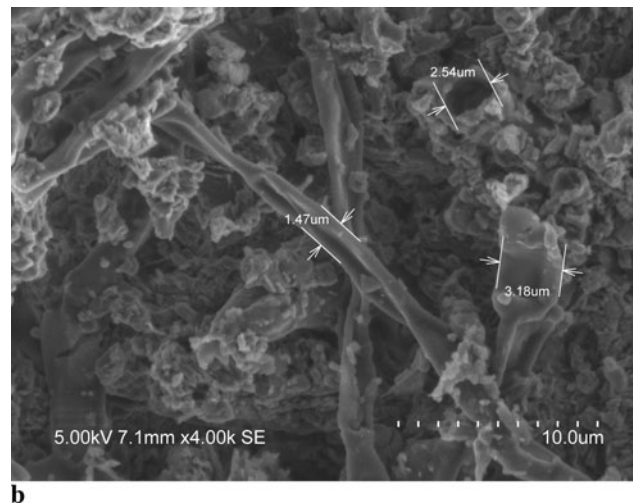
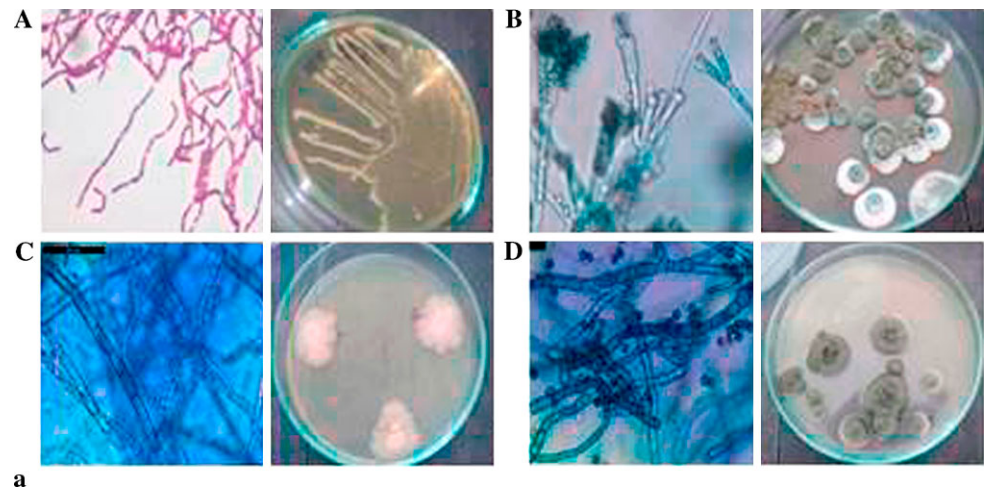
crease the solubility of the mineral phases in both basaltic rocks and basaltic glass [23, 40]. Furthermore, in experimental studies on microbial and lichenous weathering of minerals both in soil and stone substrates, biological attack has been found to be highly selective according to mineral substrate [22, 23]. Gleeson and coworkers [41], for instance, found that the presence of specific bacterial ribotypes (or species) was correlated specific chemical elements in the minerals constituting the rock substrate. It is therefore not unexpected that in the biocolonized Lalibela stone samples, deep surface etching and dissolution of mineral surfaces eventually leading to the collapse of the mineral framework appears to concentrate particularly on clinopyroxenes and Fe–Ti oxides (Figs. 8e, 8f, 8g). EDS analysis confirms the presence of Fe and Mg depletion in biologically attacked clinopyroxenes (Fig. 8e). This is in agreement with results from experimental studies on lichen-induced weathering of rocks of basaltic composition where dissolution of pyroxenes (coupled with that of olivines and Ca-plagioclases), have indeed resulted in a significant release of Fe and Mg followed by Ca and Al with subsequent precipitation of poorly ordered iron oxides and calcium oxalates [42, 43]. In Lalibela, though, oxalate compounds (i.e., weddellite), have only rarely been detected by XRD analysis and, when found, usually display low crystallinity. This could be related not to their overall absence but rather to their low degree of crystallinity as it is well known that weathering induced by lichens is often associated with the presence of noncrystalline or poorly-ordered secondary products [44]. In the cases examined, it has to be noted that an additional limiting factor for the precipitation of the most common oxalate crystalline compounds in lichen-induced rock weathering, i.e., Ca-oxalate, may have been also the relatively scarce availability of Ca ions.

5 Conclusions

Notwithstanding the already recognized important weathering role played in Lalibela by structurally related decay factors such as the presence of anthropic and/or naturally caused complex network of fractures (respectively due to the church carving itself and to the intense seismic activity of the region) and by the zeolitic and smectitic mineral components of the stone with their enhanced water absorption capabilities, the combined microscopical/chemical study highlights for the first time the major role played by epilithic and endolithic lichen colonization in the surface weathering of the Lalibela stones.

Lichen induced biodeterioration operates both via biogeophysical (hyphae contraction/swelling) and biogeochemical (acidolysis/dissolution and metal complexation) processes. Metal extraction (Fe, Mg, Al) as a source of energy and as a nutrient supply seems to particularly active on

Fig. 9 Microbiological analyses. (a) Macroscopic and microscopic features of predominant isolated strains from Lalibela biocolonized volcanic rock. (a) *Bacillus* sp. (TSA), (MEA), (b) *Penicillium* sp. (MEA), (c) *Cladosporium* sp. (MEA), (d) sterile micelia (MEA); (b) microbiological contamination (LV-SEM image)



clinopyroxene minerals. These decay processes act synergistically in causing severe desegregation of the stone fabric with the inglobation of mineral fragments from the stone substrate into the growing biological patina.

The high porosity of the volcanic scoria deposits in Lalibela coupled with their mineralogical heterogeneity (which may produce bacterial communities with unprecedented richness of species) provides the most favorable conditions for lichen and bacterial colonization and associated bio-induced decay. Once established, these patinas may act as preferential sites for water absorption/retention further accelerating both bio and/or salt weathering mechanisms.

It is therefore clear that the biological patinas do not play a protective role as it has been suggested on other lithologies [45] but, instead, should be removed as soon as possible with the correct biocide treatments as part of a comprehensive conservation program for the preservation of the Lalibela unique monumental site.

Acknowledgements We would like to thank the Ethiopian government for granting permission to one of the authors (A.K.) to collect

samples from the Lalibela monuments for the analytical campaign. N.S. would like to gratefully acknowledge the financial support to the HERCULES Laboratory (where the BSEM + EDS analysis were made) from the EEA Grants (Iceland-Lichtenstein-Norway).

References

1. UNESCO, Rock Hewn Churches, Lalibela (Ethiopia), UNESCO mission report C18, pp. 1–45 (2007)
2. R. Pik, C. Deniel, C. Coulon, G. Yirgu, C. Hofmann, D. Ayalew, J. Volcanol. Geotherm. Res. **81**, 91 (1998)
3. L. Beccaluva, G. Bianchini, C. Natali, F. Siena, J. Petrol. **50**(7), 1377 (2009)
4. C. Natali, L. Beccaluva, G. Bianchini, F. Siena, Earth Planet. Sci. Lett. **312**, 59 (2011)
5. A. Asrat, Y. Ayalew, J. Afr. Earth Sci. **59**, 61 (2011)
6. S.M. Berhe, B. Desta, M. Nicoletti, M. Teferra, J. Geol. Soc. Lond. Spec. Publ. **144**, 213 (1987)
7. B. Zanettin, Atti Accad. Naz. Lincei, Mem. Lincee. Sci. Fis. Nat. **1**, 155 (1992)
8. F. Sani, G. Moratti, M. Coli, P. Laureano, L. Rovero, U. Tonietti, N. Coli, Ital. J. Geosci. **131**(2), 171 (2012)

9. G. Delmonaco, C. Margottini, D. Spizzichino, in *Protection of Historical Buildings (PROHITECH 09)*, ed. by F. Mazzolani (Taylor & Francis, London, 2009), p. 137
10. G. Delmonaco, C. Margottini, D. Spizzichino, *Geol. Soc. Lond. Eng. Spec. Publ.* **23**, 131 (2010)
11. A. Renzulli, F. Antonelli, C. Margottini, P. Santi, F. Fratini, *J. Cult. Herit.* **12**, 227 (2011)
12. P. Laureano, Conservation action plan for the rock hewn churches in Lalibela. WMF-UNESCO/IPOGEA, Final report (2008)
13. TEPRIN, Shelters for five churches in Lalibela project. Tender dossier: Geotechnical Survey report (2002)
14. UNESCO, State of conservation of World Heritage properties inscribed on the World Heritage List, WHC-09/33.COM/7B.Add (2009)
15. C. Ascaso, J. Wierzbos, *Bot. Acta* **107**, 251 (1994)
16. N. Schiavon, *Geol. Soc. Lond. Spec. Publ.* **205**, 195 (2002)
17. N. Schiavon, in *Stone Cleaning and the Nature, Soiling and Decay Mechanisms of Stone*, ed. by R.G.M. Webster (Donhead, London, 1992), pp. 258–267
18. N. Schiavon, in *Conservation of Stone and Other Materials*, ed. by M.J. Thiel (E. & F. Spon, London, 1993), pp. 271–279
19. N. Schiavon, G. Chiavari, D. Fabbri, G. Schiavon, in *Conservation of Monuments in the Mediterranean Basin*, ed. by V. Fassina, H. Ott, F. Zezza (Balkema, Venice, 1994), pp. 43–51
20. N. Schiavon, G. Chiavari, G. Schiavon, D. Fabbri, *Sci. Total Environ.* **167**, 87 (1995)
21. J.M. Arocena, T. Siddique, R.W. Thring, S. Kapur, *Catena* **70**, 356 (2007)
22. J.K. Carson, L. Campbell, D. Rooney, N. Clipson, D.B. Gleeson, *FEMS Microbiol. Ecol.* **67**, 381 (2009)
23. S.E. Favero-Longo, D. Castelli, O. Salvadori, E. Belluso, R. Piervittori, *Int. Biodeterior. Biodegrad.* **56**, 17 (2005)
24. G.M. Ingo, G. Bultrini, T. de Caro, C. Del Vais, *Surf. Interface Anal.* **30**, 101 (2000)
25. G.M. Ingo, E. Angelini, G. Bultrini, T. De Caro, L. Pandolfi, A. Mezzi, *Surf. Interface Anal.* **34**, 328 (2002)
26. G.M. Ingo, I. Fragalà, G. Bultrini, T. de Caro, C. Riccucci, G. Chiozzini, *Thermochim. Acta* **418**, 53 (2004)
27. G. Padeletti, G.M. Ingo, A. Bouquillon, S. Pages-Camagna, M. Aucouturier, S. Rohers, P. Fermo, *Appl. Phys. A* **83**, 475 (2006)
28. N. Schiavon, A. Candeias, T. Ferreira, M. Da Conceição Lopes, A. Carneiro, T. Calligaro, J.P. Mirao, *Archaeometry* **54**, 974 (2012)
29. A. Santos Silva, T. Cruz, M.J. Paiva, A.E. Candeias, P. Adriano, N. Schiavon, J.A.P. Mirao, *Environ. Earth Sci.* **63**, 1641 (2011)
30. N. Schiavon, G.A. Mazzocchin, F. Baudo, *Environ. Geol.* **56**, 767 (2008)
31. N. Schiavon, in *Conservation Science for the Cultural Heritage: Applications of Instrumental Analysis*, ed. by E.A. Varella (Springer, Berlin, 2013), pp. 249–257
32. Z.T. Bieniawski, *Engineering Rock Mass Classifications* (Wiley, New York, 1989)
33. D. Ayalew, G. Yirgu, R. Pik, *J. Afr. Earth Sci.* **29**, 381 (1999)
34. J. Wierzbos, C. Ascaso, *Clays Clay Miner.* **44**, 652 (1996)
35. P. Adamo, P. Violante, *Appl. Clay Sci.* **16**, 229 (2000)
36. N. Schiavon, L.P. Zhou, *Environ. Sci. Technol.* **30**(12), 3624 (1996)
37. N. Schiavon, *Environ. Geol.* **52**, 399 (2007)
38. WUB Consult, Environmental Impact Assessment of the resettlement project in Lalibela. UNESCO (2011)
39. J. Chen, H.P. Blume, L. Beyer, *Catena* **39**, 121 (2000)
40. C.S. Cockell, P. van Calsteren, J.F.W. Mosselmans, I.A. Franchi, I. Gilmour, L. Kelly, K. Olsson-Francis, D. Johnson, *Chem. Geol.* **279**, 17 (2010)
41. D. Gleeson, N. Kennedy, N. Clipson, K. Melville, G. Gadd, F. McDermott, *Microb. Ecol.* **51**, 526 (2006)
42. I.K. Iskandar, J.K. Syers, *J. Soil Sci.* **23**, 255 (1972)
43. D. Jones, M.J. Wilson, J.M. Tait, *Lichenologist* **12**, 277 (1980)
44. M.J. Wilson, D. Jones, in *Residual Deposits: Surface Related Weathering Processes and Materials*, ed. by R.C.L. Wilson (Blackwell, London, 1983), pp. 5–12
45. M.R.D. Seaward, C. Giacobini, M.R. Giuliani, A. Roccardi, *Int. Biodeterior. Biodegrad.* **25**, 49 (1989)